SPACE TELESCOPE SCIENCE INSTITUTE
Operated for NASA by AURA

WFC3 Instrument Science Report 2008-21

WFC3 TV3 Testing: UVIS Channel Calibration Subsystem Performance

S. Baggett
October 17, 2008

ABSTRACT

*This report summarizes the behavior of the WFC3 calibration system in the UVIS channel, based upon data acquired during thermal-vacuum level tests performed in 2008 with the UVIS-1' flight detector. The results are evaluated in light of the calibration system requirements. Tungsten: the new lamps satisfy the flux requirement of at least 16.7 e^-/s/pix for all filters except in FQ436N and FQ437N (~9 and ~6 e^-/s/pix, respectively, with tungsten lamp 3). Overall, the lamp output was found to be 1-2% higher when operated on side 1 of the instrument than it was on side 2. Of the four tungsten lamps, #4 has the highest flux, followed by #2 and #3; lamp #1 has the lowest output. Specifically, #3 is about 15-20% fainter than #4 and about 10-15% brighter than #1. A full evaluation of the short- and particularly long-term stability requirements will require more data. However, based on the flatfields obtained during TV3, the short-term stability requirement is met in the majority (80-90%) of cases. The long-term stability will not be met if the TV3 decline rates continue (typically 1-3% in 10-40 days), but there is some evidence that the rate of decline may be slowing. Over the large scale, the tungsten flatfields meet the uniformity specification (< factor of two over the full field of view) in all but three filters (*F410M, F657N, and F658N*); these exceptions, however, are due to the filters, not the lamps. Lamp lifetimes in the lab were 1960 hrs each, with some parts lasting more than 3000 hrs; if the flight lamps last this long, they will easily meet the lifetime requirement. Deuterium: the lamp satisfies the calsystem flux requirement except when used with FQ387N, FQ436N, and FQ437N (~16, ~14, and ~11 e^-/s/pix, respectively). While the short-term stability is found to be generally good, the lamp will not meet the long-term requirement, having declined by 2-10%,*

depending upon filter, during the ~40 days of TV3. Over large scales across the FOV, the deuterium flatfields meet the uniformity specification. There are, however, small scale features (10-20 pix) where the flux can vary by more than a factor of two - but these features are due to residue on the CCD window, not the lamp.

Introduction

The calibration subsystem (calsystem) in WFC3 has been designed to provide uniform internal flatfield illumination across the field of view of both channels. While not employed directly in the calibration pipeline, the internal flatfields are used to determine the corrections necessary to update the ground flatfield datasets for use on-orbit, as well as monitor for any on-orbit flatfield changes and provide a means for assessing the health of the instrument. Visible flux is provided by one of four Carley tungsten bulbs, procured and installed after TV2 testing in 2007 and described in more detail in the Flux Levels portion of the Tungsten Exposures section. Two tungsten bulbs are nominally assigned to each WFC3 channel - one as primary and one as the backup - although any lamp can be configured to be used with either channel. Currently, the primary and backup for the UVIS channel are lamps #3 and #1, respectively; the backup bulb is accessible in the proposal software (APT) via special commanding. UV flux is provided by a deuterium lamp (D2), for which there is no spare. For the UVIS channel, light from the D2 lamp or the tungsten lamp assembly is relayed to the detector through a hole located in the center of the UVM2 mirror (the hole is located at the pupil image of the OTA central obscuration).

The requirements for the calsystem specify that it must provide 1) illumination uniform to better than a factor of two over the field of view, 2) stability over hour (<1%/pixel) and year (<5%) timescales, and repeatability (over a year) to +/- 50K color temperature, and 3) flux from 200-2000nm at the level of at least 10K e^- in 10 minutes (~16.7 e^-/s/pix) for all spectral elements. This report summarizes the characteristics of the calsystem data taken during 2008 thermal-vacuum instrument-level testing and compares the results to the specifications.

Observations and Analysis

The UVIS calsystem flatfields analyzed here were taken via four different TV3 programs: calsystem flatfields (OPUS image names iu23*), the science monitor (iu28*), the system functionals (i61g*), and the aliveness portion of the system functional (i9v9*). The images were acquired at the nominal gain (1.5 e^-/DN) and bias offset (~2500DN) settings, in full-frame, unbinned, four-amp readout mode. The majority of the data were taken with the detectors at -83C; some were also obtained during ambient testing, with the detectors at

about -50C, but those are not considered in this report. While most data were acquired with lamp 3, a small amount of data were taken with the other tungsten lamps in order to assess the relative illumination levels. The deuterium exposures were all taken at medium current to maximize the lifetime of the lamp as high current has been shown to age the lamp faster than medium (Baggett & Quijada, 2003). All images were processed through calwf3, performing the overscan correction (BLEVCORR) only and using the most recent versions of CCDTAB and OSCNTAB available at the time (r6p1618ci_ccd.fits and q911321oi_osc.fits, respectively).

UVIS Tungsten Exposures

Image Features

Two typical UVIS calsystem flatfields are shown in Figure 1; images of TV3 tungsten flatfields for each filter are available in the Calsystem Flatfield Atlas (Sabbi, 2008).

Figure 1: Full-frame, four-amp readout tungsten calsystem flatfields in F390W and F606W, left and right respectively, shown with an inverted greyscale stretch (+/-20%). Quadrants in this figure, and all subsequent figures, are shown in the nominal position (labelled A,B,C,D).

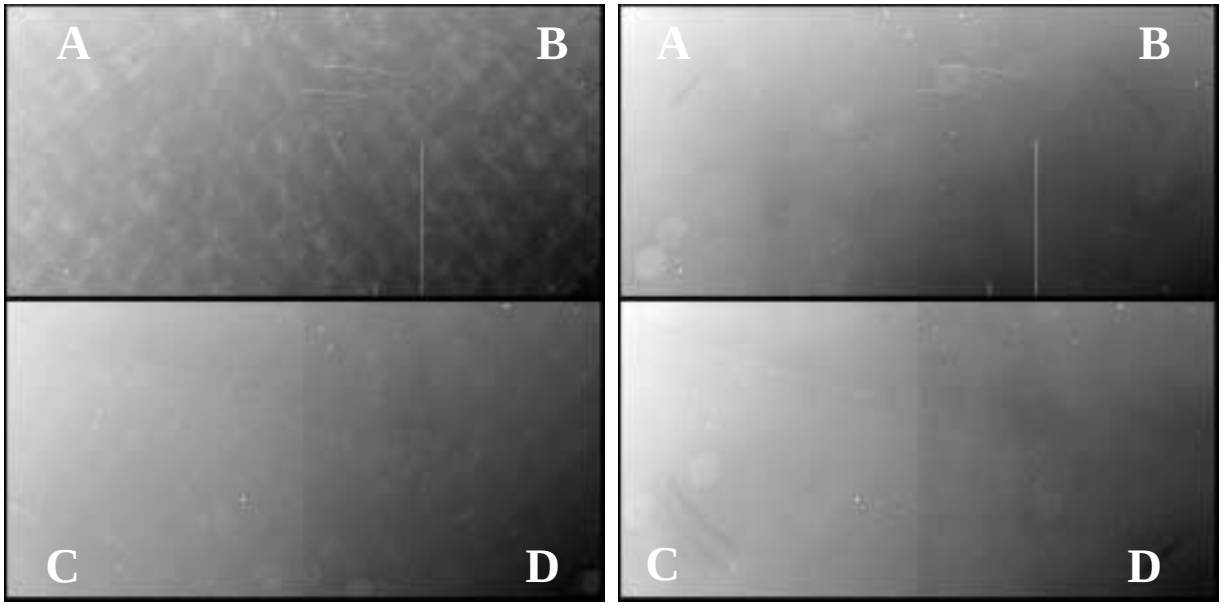

- As discussed in previous reports (Baggett 2008 and references therein), the prominent glints in amps B and C are gone, thanks to painting of the baffle tube between the filter wheel assembly and the shutter. In addition, a flare in quadrant A, extending into a faint diamond shape which spanned the field of view from the A quadrant to the D quadrant is gone as well (Brown, 2008), the problem traced to glints from the UVIS detector housing which has now been masked.

- There is an overall gradient across the field of view, from a low near the outer corner of quadrant A, to a high near the outer corner of quadrant D (~30% across entire FOV). This is an artifact of the optical design of the UVIS channel: the detector is tilted such that the amp A corner is further from, and amp D is closer to, the hole in the M2 mirror through which the calsystem beam passes (G. Hartig, private communication).
- The outer corners of each quadrant show small arc-shaped glints at the level of a couple percent. These were present in earlier ambient data taken with UVIS-2 as well as in earlier data taken with UVIS-1. They are not visible in external flatfields, though similar arc features have been seen in images containing (heavily exposed) point sources.
- As expected, narrowband images, particularly at redder wavelengths, show fringing due to interference within the detector layers. The fringes become closely spaced within a large circular area in quadrant D, a symptom of rapidly-changing thickness (and sensitivity) of the CCD detection layer.
- Extended donut-like artifacts, about 150-250 pixels in diameter, can be seen in some flatfields, due to particles on the filter (e.g., F606W image in Figure 1). Smaller spots (~10-40 pixels in diameter) are due to dust or condensation residue on the CCD windows; the effects of the latter have been discussed in detail in Brown et al. (2008).
- UV flatfields, both tungsten and deuterium, have a characteristic crosshatch pattern, a result of the chip manufacturing process.
- A small number of flatfields show anomalous features due to the specific filter (see Sabbi, 2008, for a complete atlas of calsystem flats). These include FQ387N, with a diffuse horizontal band of light, F410M, with scattering from beveled filter edges, F657N and F658N (horizontal and vertical bands of scattered light which can be 10's of percent higher than surrounding level), and some faint scattered light in FQ508N/FQ575N and FQ619N/FQ750N. The significantly higher f-ratio of the calsystem beam accentuates these features; that is, they are not visible in the flatfields with the HST-like beam from the external stimulus.

Overall, the tungsten flatfields meet the uniformity specification, with the exception of F410M, F657N, and F658N, where flux levels in small regions of the flatfields can exceed a factor of two over the overall level. However, in these cases, the failure to meet the requirement is not within the calsystem but due to the filter.

Flux Levels

The tungsten bulbs used in ground tests *prior* to TV3 in 2008 were Welch Allen incandescent lamps filled with krypton. Despite having survived burn-in and liftetime tests and being rated for ~1500 hrs of use, once assembled into the WFC3 calsystem only a small fraction of that lifetime was achieved. Tungsten flatfields from TV2 showed dramatically declining count-rates along with declining current levels at lamp turn-on, with two lamps burning out before the end of the test (Baggett, 2008). Evaluation of the failed flight bulbs revealed that cracks had developed in the epoxy holding the lamps and leads to their rings (C. Powers, private communication). Once a crack develops, the tungsten oxidizes and

begins to darken the bulb envelope; once the gas within the glass envelope is gone, the filament burns out.

The bulbs in the spare tungsten assembly were subsequently evaluated and found to be suffering from similar problems, including bent leads and even broken glass around the leads (T. Delker & M. Kilpatrick, private communication). In addition, one of the four spare bulbs visibly darkened after it was turned on in the lab. As a consequence, new tungsten lamps were procured from Carley Lamps in California, and installed in new flight and spare tungsten lamp assemblies which were subsequently used for TV3. While functionally the same as the old bulbs (e.g., operating at the same voltage, providing similar spectral output), the new Carley bulbs feature a variety of improvements, including higher quality glass, more uniformly spaced thicker tungsten filaments, heavier concave seals at the envelope base to inhibit cracking, and a more robust design of the leads and filament/lead transition (to eliminate bubbling in the glass, thought to be a contributing factor in the prior lamp failures), along with special attention to the lead welding and filament construction (Powers, 2007). Additional inspections were performed to specifically check for issues like poor backfill, bent leads, or cracks that could lead to leaks in the envelope. Furthermore, the procedures and tools for installing the lamps into the tungsten lamp assembly were revised to minimize any unnecessary mechanical stress on the bulbs during the assembly build-up (M. Kilpatrick, private communication).

Based on lab tests of 15 Carley bulbs from the same lot as the new flight/spare bulbs, the lifetime for stable operations of a given lamp is estimated to be at least 1960 hrs (Powers, 2008), with a 50/50 chance that a lamp will last for 3300 hrs. These are relatively conservative estimates, as any reweld event[1] was considered the end of stable operational life for the lamp, even though the lamp would still provide flux after a reweld. During the lifetime testing, four of the fifteen lamps survived more than 3500 hrs (one survived to nearly 4500 hrs).

Table 3 in Appendix A lists the UVIS-1' tungsten lamp countrate results; tabulated are filter name, lamp number, CCD temperature as given by the IUVDETMP header keyword, day of year that the image was taken, TV number of the image (tvnum), median count-rates in chip 1 (quads A/B), in chip2 (quads C/D), and flux ratio of the flat as referenced to the first flat taken in that filter/lamp/temperature group. All count-rates have been converted to e^- using gain = 1.5 e^-/DN. Since quad filter flatfields contain different bandpasses in each quadrant of the WFC3 field of view, the flux levels were measured in

1. Tungsten grain growth on the filament is considered the primary failure mechanism in the new lamps, eventually leading to a runaway hot spot which either rewelds or causes the filament to burn out (Powers, 2008). The lab tests showed that new lamps are more likely to have rewelds than burn outs.

the central 1000x1000 pixels within those quadrants; these results are shown in Table 4 in Appendix A.

As the countrate tabulated in the Appendices show, the vast majority of filters meet the flux level spec (>16.7 e^-/s/pix). UV filters with low tungsten count-rates generally have sufficient flux with the D2 lamp; however, neither lamp meets the flux specification for three filters: FQ387N, FQ437N, and FQ437N. The first sees highest illumination level with the D2 lamp, at ~11 e^-s/pix while the last two have levels of ~9 and 7 e^-s/pix, respectively, with the tungsten lamp #3. However, these flux levels are sufficient to allow the acquisition of flats with S/N of ~100 in 15-25 min.

The vast majority of flatfields during TV3 were taken with the side 2 electronics (MEB2), with typically only one flatfield per filter taken with MEB1. However, there were two quad filters for which significant numbers of flatfields were required in order to achieve the desired total flux level[1] and for which there are 4 or more images per side. As the count-rates in Table 3 in Appendix A show, the lamp output is 1-2% higher when operated with MEB1 than with MEB2, similar to what was found with the older Welch-Allen bulbs with UVIS-2 during TV2 (Baggett, 2008).

To evaluate the output of the tungsten bulbs relative to each other, flatfields in a small number of filters were taken with each of the 4 lamps. The results are summarized in Table 1 in the form of quadrant statistics of image ratios of #3 to each of the other lamps in turn (#3 was the primary lamp for the UVIS channel during TV3 and is designated as such for on-orbit use as well). Some minor clipping has been done on the images (3x3 sigma) to filter out a small number of bad columns/rows. Depending upon the wavelength regime, lamp 3 is 10-15% brighter than lamp 1, 1-15% fainter than lamp 2, and about 15-20% fainter than lamp 4. Image ratios showed that there are some low-level, large scale differences in the illumination patterns of the lamps (<1% across several thousand pixels); this would, of course, need to be taken into account if on-orbit calsystem flatfields are taken with a lamp other than #3.

1. Each quad filter consists of 4 different bandpasses, one per amp, with different countrate levels. Flatfield exposure times were chosen so that none of the bandpasses saturated; however, in some cases, this meant that extra iterations of flatfields were needed in order to achieve the minimum total exposure level in the slowest bandpass.

Table 1. Tungsten lamp 3 output relative to the other three tungsten lamps.

lamp	filter	A quadrant		B quadrant		C quadrant		D quadrant	
		mean	sdev	mean	sdev	mean	sdev	mean	sdev
1	F438W	1.145	0.009	1.135	0.009	1.153	0.009	1.143	0.008
1	F555W	1.145	0.01	1.137	0.009	1.155	0.009	1.147	0.009
1	F814W	1.124	0.01	1.118	0.01	1.135	0.009	1.129	0.009
2	F438W	1.009	0.007	1.009	0.007	1.005	0.007	1.005	0.007
2	F555W	0.955	0.007	0.957	0.007	0.95	0.007	0.953	0.006
2	F814W	0.869	0.007	0.872	0.007	0.863	0.007	0.868	0.006
4	F438W	0.861	0.006	0.859	0.006	0.866	0.006	0.863	0.006
4	F555W	0.858	0.007	0.855	0.006	0.866	0.006	0.862	0.006
4	F814W	0.822	0.007	0.818	0.007	0.831	0.007	0.827	0.006

Tungsten lamp repeatability

Both short- and long-term stability requirements exist: <1% over 1 hour and <5% over 1 year. Most flatfields in a given filter are spaced days apart; however, a small set of 400x400 subarray tungsten flatfields acquired for other purposes do exist, with pairs of frames taken on very short timescales: 1-7 minutes apart. Image ratios of these pairs are featureless and as shown in Table 2, the flux levels are generally the same to better than 1%, however, there are two pairs where the difference is closer to 2%, violating the short-term specification.

On a slightly longer short timescale, there were about 15 pairs of full-frame tungsten flat-fields taken less than 24 hours apart (see Table 3 in Appendix A). In all but two cases, the tungsten lamp output was found to repeat to better than 0.5%; image ratios were feature-less, except for the very shortest exposures, when the normal, very low-level (<0.2%) shutter travel features can be seen (right image in Figure 2).

The two exceptions to acceptable repeatability were part of two triplet sequences; that is, three F343N flatfields taken back-to-back, one set on day 93 and one set on day 95 (tvnum 55569-55571 and 56516- 56518). On both days, the flux level in the third flatfield was lower than in the first two flatfields by about the same amount, ~12%. There was no apparent cause for either discrepancy; the image format and commanded exposure time (2000 sec) were identical. The triplets of F343N flatfields were embedded in an SMS which acquired a total of 20 tungsten images in a variety of filters as well as two bias images, none of which showed any problems. Image ratios of each low F343N flatfield to

one of the normal F343N flatfields were featureless; in addition, the countrate of a F343N calsystem flatfield taken ~5 days after the first low-flux F343N flatfield was almost back to the original, higher signal level; there were no more F343N flatfields taken after the last low-flux F343N image. An analysis of the SMS command blocks and the image telemetry revealed no anomalies that could account for the lower flux (T. Wheeler and I. Dashevsky, private communication). In contrast to the F343N case, three sets of eight images each taken for the quad2 filter (tvnums 54271-54278, 56214-56221, and 56793-56800, see Table 3 in Appendix A) showed flatfield fluxes in agreement to better than 1%.

Table 2. Repeatability of subarray tungsten flatfields.

filter	exptime	tvnums	date-obs	time-obs	time-obs	image ratio statistics		
						mean	stdev	median
f438w	300.	49374/75	Mar 7, 2008	21:57:52.05	22:05:04.05	0.982	0.006	0.982
f814w	1.6	49376/77	Mar 7, 2008	22:12:04.05	22:13:09.04	1.003	0.007	1.003
f438w	300.	49430/31	Mar 8, 2008	02:12:54.05	02:20:06.05	0.991	0.006	0.990
f814w	1.6	49432/33	Mar 8, 2008	02:27:06.05	02:28:11.04	1.006	0.007	1.005
f438w	300.	49504/05	Mar 8, 2008	06:17:50.05	06:23:33.06	0.988	0.006	0.988
f814w	1.6	49506/07	Mar 8, 2008	06:29:36.07	06:30:41.06	1.007	0.007	1.006

Verification of the long-term flux stability will require additional data at a later time; however, initial indications from the data currently available imply that it may not be satisfied. As can be seen in the ratio column in Table 3, overall there has been a small decline in output in most filters over the course of TV3. Many filters show a reduction in output 2-3% over the 25-40 days; if the decline should continue at this rate, the lamps will not meet the long-term requirement of <5% change over 1 year. However, some filters (e.g., F350LP, F555W, F814W) showed small increases in flux near the end of testing; if this should signal stabilization of the lamp output, the long-term requirement may yet be met. Monitoring of the lamp output will be continued through the upcoming Servicing Mission Orbital Verification and the observing cycles beyond.

In addition, image ratios of flatfields within a given configuration (same filter and operating temperature) were examined. While most were generally featureless, there were occasional occurences of the low-level ‘bowtie’ phenomenon noted in previous ground test campaigns (Baggett, 2008; Bushouse & Lupie, 2005). More common at off-nominal CCD operating temperatures, the features do sometimes occur at the nominal operating temperature (see left image in Figure 2) at very low levels; they are not related to the calsystem but are attributed to a QE hysteresis-type effect within the chips themselves.

Figure 2: At right is a hard stretch (+/-1%) of an image ratio of two F814W images taken within 14 hours of each other, illustrating low-level shutter edge effects (the slanted lines which appear to emanate from the upper right, B amp corner). At left is an image ratio of two F555W images taken about 26 hours apart, showing the CCD 'hysteresis' effect. Stretch is +/-10%.

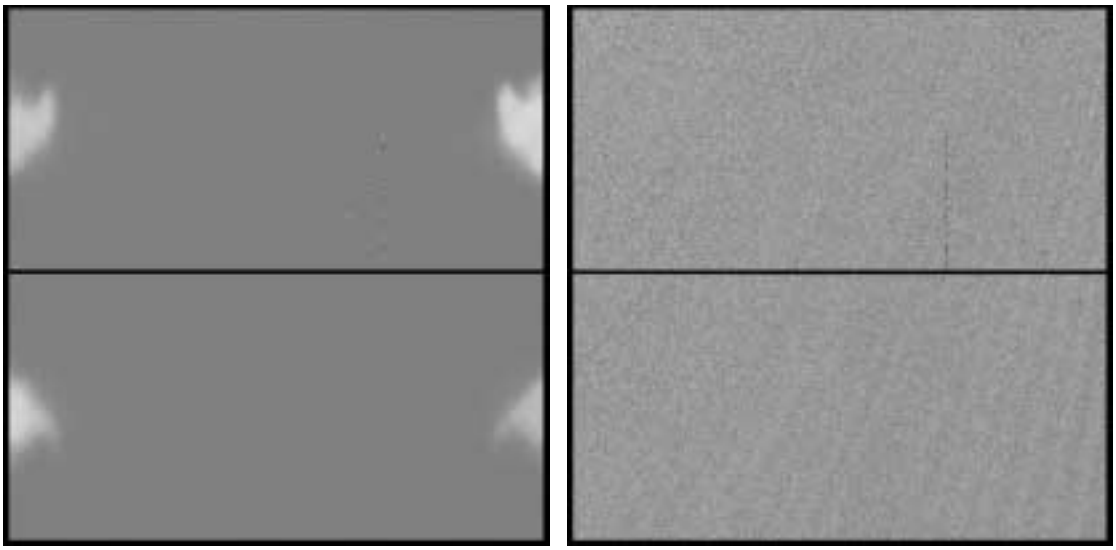

UVIS Deuterium Exposures

Image Features

As noted in the previous TV campaign, the deuterium flatfields are now relatively flat in comparison to the images from the first ground testing which showed 5-10x gradients across the field of view from C quadrant up through B quadrant. Figure 3 shows two deuterium flatfields from TV3, the left image taken with F218W and right with F390W. The characteristic background cross-hatch pattern seen in all UV flatfields is present (due to the CCD manufacturing process); the features are typically a few percent peak to peak but extremely repeatable from image to image. The overall gradient across the FOV is ~5-15% though the F390W shows more of a downturn, at the level of a few 10's of percent, in the outer corners of quadrants B and D. The small dark spots in F218W are painted pinholes; on an even smaller scale (~10 pixels) are features due to an evaporated residue on the CCD window acting as a small lens. Due to the ~f/300 beam of the calsystem, these features are visible as sharp, localized blemishes; in the science beam (~f/31), they are considerably less prominent and each is spread out over a much larger chip area (the effects on science data are discussed in Brown 2008). Excluding the small spots and the extreme roll-offs at the edge which seem to be worse in redder filters, overall the deute-

rium flatfields meet the uniformity specification requiring the illumination pattern be flat to better than a factor of two across the field of view.

Figure 3: UVIS calsystem deuterium flatfields (F218W at left and F390W at right) shown in inverted stretch with scale at +/-20%.

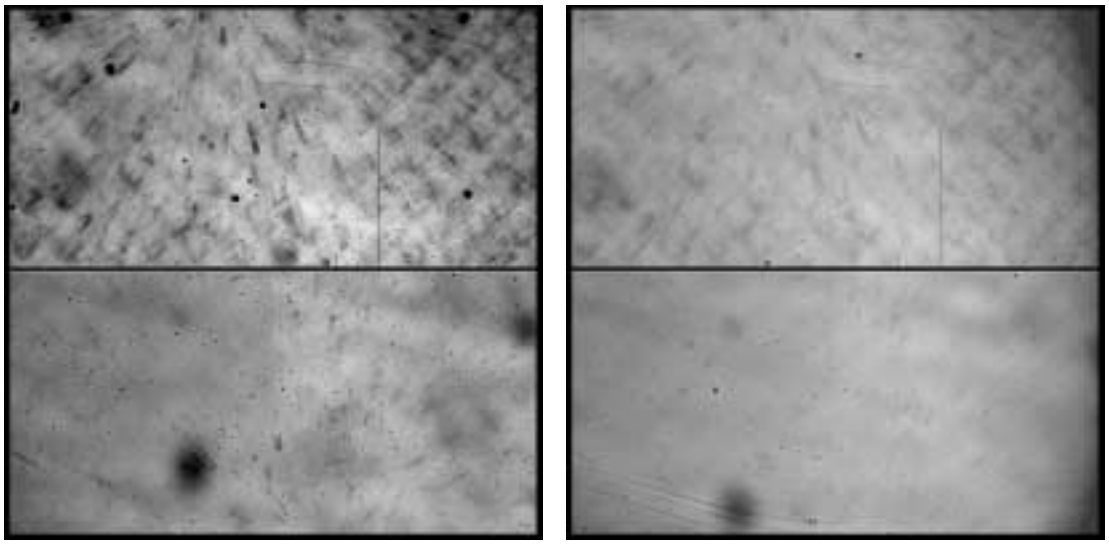

Flux Levels

The flux levels measured in the TV3 deuterium flatfields are provided in Table 5, 6, and 7 in the Appendix, for full-frame images, subarrays, and quad filters, respectively. Listed are filter, exposure time, instrument side, CCD temperature (from IUVDETMP keyword), day of year the image was taken, TV image number, median in each chip (or in central 400x400 region of the appropriate amp for the quad filters), and ratio of the median to the level in the first image of a given filter. All exposure levels have been converted to e^-/s/pix using 1.5 e^-/DN. The flux requirement is met for all but three of the quad filters: FQ387N, FQ436N, and FQ437N (~16, ~14, and ~11 e^-/s/pix, respectively). The specification could be met by operating the deuterium lamp at the high current setting (doubling the count-rate); however, lamp lifetime test results showed that the medium current setting minimized degradation in lamp performance and provided the most stable short- and long-term throughput (ISR 2003-11). Lamp operations are expected to be restricted to medium current only.

Deuterium Lamp Repeatability

Based upon a small number of full-frame and subarray flatfields taken back-to-back (see Table 5 and 6 in the Appendix) and excluding the first one or two exposures in each subarray set (where the lamp is still warming up), the deuterium lamp output is repeatable to better than 1%. There were occasional lamp turn-on delays, when the D2 failed to fire during the nominal 2 seconds; it would eventually turn on within a few minutes (1-10). Obviously any flatfield being taken during that time has no D2 flux; subsequent flatfield exposure levels after the delayed turn-on exhibited the expected flux levels. Programs using the D2 lamp on-orbit will be structured so as to be relatively immune to the occasional loss of the first flat in a D2 set.

On a large scale across the entire FOV, most image ratios of the D2 flats are flat to 1% or better but there are significant localized deviations (up to a factor of two) at the cores of the features due to the residue on the CCD window. Many filters also show evidence of a broad, diffuse wavelike pattern, up to ~2% peak-to-peak in F218W, less in the redder filters, which varied over time. Figure 4 shows image ratios for F218W (left) and F336W (right) using a hard stretch of +/- 5%. In each case, for all flats in the given filter a ratio was taken to the earliest flat in the set. The F218W files were taken March 6 to April 13 and the F336W data were taken March 18 to April 5. There were significantly more D2 flats taken in F218W than in other filters, as it was part of the system functional and science monitor programs, as well as the calsystem program. As the figures show, the features in some of the F218W are stronger than in F336W; and the finer timesampling in F218W illustrates how the feature strength can vary significantly, from sub 0.1% up to ~2% peak-to-peak. While the cause of this pattern and its variation is unknown, given that the pattern varies smoothly across the gap, occurs in multiple filters, and it does not appear in the tungsten flats, it is likely related to the D2 lamp itself, e.g., on the bulb window. If the variations continue on-orbit, this will limit the degree to which the calsystem flats can be used to monitor flatfield changes.

Figure 4: Deuterium flatfield image ratios, F218W at left, F336W at right. Both are shown with a hard stretch of +/- 5%.

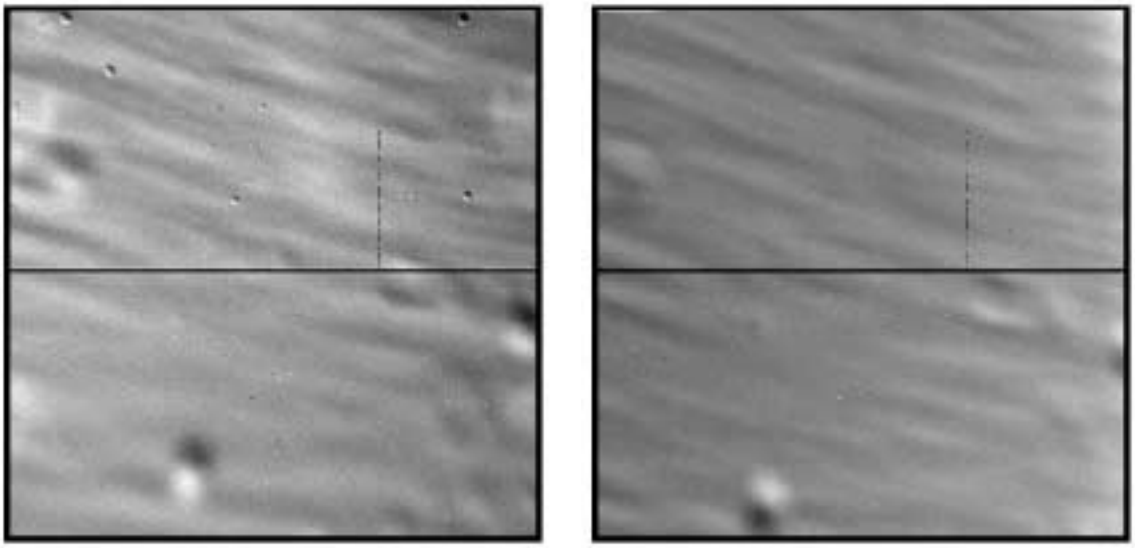

Figure 5: Cuts through deuterium flatfield image ratios using F218W (left) and F336W (right); each cut is an average of 150 columns through quadrant D, plot scale is +/-2% in all cases. Time range for F218W spans March 6 (bottom plot) to April 13 (top plot); F336W data spans March 18 (bottom) to April 5 (top).

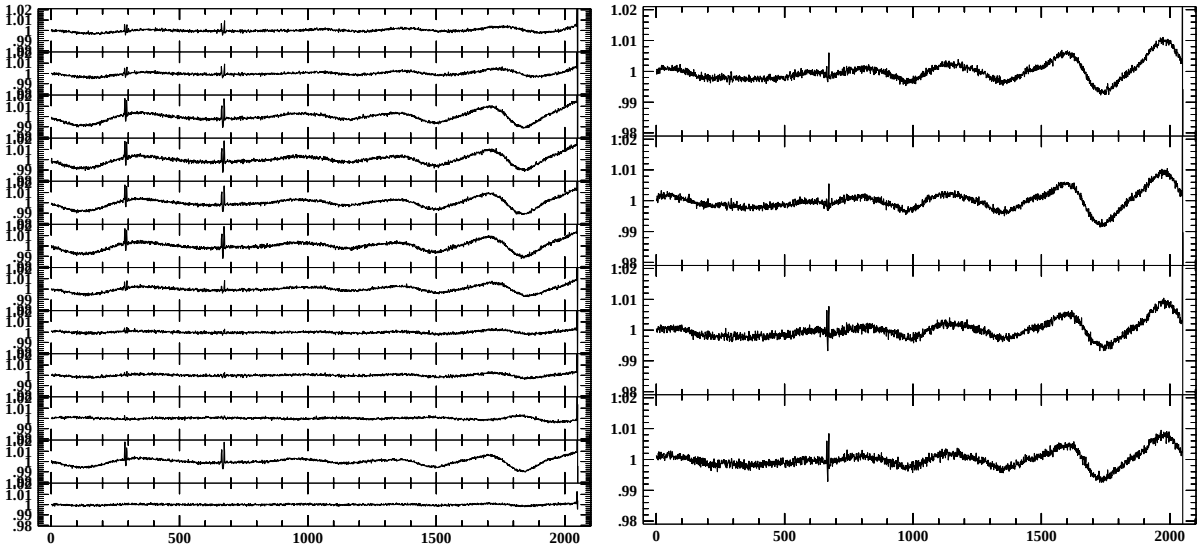

Conclusions

The WFC3 calsystem flatfields from TV3, obtained with the UVIS-1' have been analyzed. Details of the illumination patterns were discussed, count-rates tabulated, and image repeatability investigated. The results have been evaluated in light of the uniformity, flux, and long-term stability specifications.

Acknowledgments

Thanks are due to the extended WFC3 team at STScI, Goddard, and Ball Aerospace, who supported the thermal vacuum tests.

References

Baggett, S., “WFC3 TV2 Testing: Calibration Subsystem Performance,” Instrument Science Report 2008-01, 2008.

Baggett, S., and Quijada, M., “Lifetime Test of a Deuterium Lamp for the WFC3 Calibration Subsystem,” WFC3 Instrument Science Report 2003-11, 2003.

Brown, T., “WFC3 TV3 Testing: UVIS Channel Glints,” WFC3 Instrument Science Report 2008-07, 2008.

Brown,T., Hartig, G., and Baggett, S., “WFC3 TV3 Testing: UVIS Window Contamination,” WFC3 Instrument Science Report 2008-20, 2008.

Bushouse, H., and Lupie, O., “WFC3 Thermal Vacuum Testing: UVIS Science Performance Monitor,” WFC3 Instrument Science Report 2005-20, 2005.

Powers, C., “Evaluation of Carley Lamps for HST/WFC3,” internal GSFC memo, Materials Engineering Branch, Apr. 2008.

Powers, C., “Source Inspection of Carley Lamps for HST/WFC3,” internal GSFC memo, Materials Engineering Branch, Aug. 2007.

Sabbi, E., “UVIS Calsystem Photometric Filter Flat Field Atlas,” WFC3 Instrument Science Report 2008-17, 2008.

Appendix A. Calsystem Count-rates

Table 3. UVIS tungsten lamp flatfield count-rates from TV3. Listed are filtername, lamp number, CCD temperature as given by the IUVDETMP header keyword, day of year that the image was taken, TV number of the image, median count-rates in chip 1 (quads A/B), in chip2 (quads C/D), and flux ratio of the flat as referenced to the first flat taken in that filter/lamp/temperature group. All count-rates have been converted to e^- using a gain of 1.5 e^-/DN. See Table 4 for exposure levels for specific quadrants of the quad filters.

filter	L	iuv-detmp	doy	tvnum	median (e^-/s/p)		ratio
					chip1	chip2	
f200lp	3	-81.7	078	52456	31785.2	29281.5	1.00
f200lp	3	-81.7	093	55666	31774.7	29236.3	1.00
f200lp	3	-81.5	099	56760	31448.6	28951.4	0.99
f200lp	3	-81.9	104	57992	29821.0	27433.4	0.94
f336w	3	-82.1	078	52448	3.6	3.2	1.00
f336w	3	-81.7	093	55658	3.5	3.1	0.97
f336w	3	-81.9	099	56752	3.5	3.0	0.96
f336w	3	-81.9	104	57993	3.4	3.0	0.95
f343n	3	-81.7	086	53846	2.3	2.0	1.00
f343n	3	-81.7	093	55569	2.2	1.9	0.98
f343n	3	-82.1	093	55570	2.2	1.9	0.98
f343n	3	-81.9	093	55571	2.0	1.7	0.87
f343n	3	-81.7	098	56516	2.2	1.9	0.96
f343n	3	-81.9	098	56517	2.2	1.9	0.96
f343n	3	-81.9	098	56518	1.9	1.7	0.86
f350lp	3	-81.9	078	52447	33456.0	30576.3	1.00
f350lp	3	-81.9	078	52447	33456.0	30576.3	1.00
f350lp	3	-81.7	093	55657	32824.9	30156.8	0.98
f350lp	3	-81.7	093	55657	32824.9	30156.8	0.98
f350lp	3	-81.9	099	56751	32290.3	29745.8	0.97
f350lp	3	-81.9	099	56751	32290.3	29745.8	0.97
f350lp	3	-81.7	104	57994	33876.5	30955.8	1.01
f350lp	3	-81.7	104	57994	33876.5	30955.8	1.01
f390m	3	-81.7	086	53838	11.6	10.2	1.00
f390m	3	-81.9	093	55560	11.4	10.0	0.98
f390m	3	-82.1	093	55561	11.4	10.1	0.98
f390m	3	-81.7	098	56507	11.2	9.9	0.97
f390m	3	-81.7	098	56508	11.3	9.9	0.97
f390w	3	-81.5	078	52444	83.3	74.4	1.00
f390w	3	-81.9	093	55515	81.9	73.2	0.98
f390w	3	-81.7	098	56503	80.9	72.2	0.97
f390w	3	-81.7	104	57995	80.4	71.8	0.97
f395n	3	-82.1	086	53848	5.8	5.1	1.00
f395n	3	-81.9	093	55573	5.6	5.0	0.98
f395n	3	-81.7	093	55574	5.7	5.1	0.98
f395n	3	-81.7	098	56520	5.6	5.0	0.97
f395n	3	-82.1	098	56521	5.6	5.0	0.97
f410m	3	-82.1	086	53840	31.2	27.1	1.00
f410m	3	-81.5	093	55563	30.8	26.6	0.99
f410m	3	-81.9	098	56510	30.6	26.3	0.98
f410m	3	-81.7	104	57996	30.4	26.2	0.97

filter	L	iuv-detmp	doy	tvnum	median (e^-/s/p)		ratio
					chip 1	chip 2	
f606w	3	-81.9	078	52450	8870.9	7975.6	1.00
f606w	3	-81.9	078	52450	8870.9	7975.6	1.00
f606w	3	-81.7	093	55660	8741.2	7889.3	0.99
f606w	3	-81.7	093	55660	8741.2	7889.3	0.99
f606w	3	-81.9	099	56754	8657.9	7807.6	0.98
f606w	3	-81.9	099	56754	8657.9	7807.6	0.98
f606w	3	-81.9	104	58000	8647.1	7793.3	0.98
f606w	3	-81.9	104	58000	8647.1	7793.3	0.98
f621m	3	-82.1	086	53839	2900.5	2611.0	1.00
f621m	3	-81.9	093	55562	2869.1	2594.6	0.99
f621m	3	-81.9	098	56509	2843.4	2571.2	0.98
f625w	3	-81.9	078	52451	7265.7	6525.8	1.00
f625w	3	-81.7	093	55661	7152.6	6452.4	0.99
f625w	3	-81.7	099	56755	7080.3	6387.6	0.98
f625w	3	-82.1	104	58001	7086.8	6391.7	0.98
f631n	3	-81.7	088	54269	264.0	240.1	1.00
f631n	3	-81.7	096	56212	262.5	237.3	0.99
f631n	3	-81.7	099	56791	259.5	235.7	0.98
f645n	3	-81.7	078	52455	428.1	394.5	1.00
f645n	3	-82.1	093	55665	423.3	390.9	0.99
f645n	3	-81.7	099	56759	419.3	386.5	0.98
f645n	3	-81.7	104	58002	417.7	385.3	0.98
f656n	3	-82.1	078	52441	96.4	86.8	1.00
f656n	3	-81.7	093	55512	95.6	86.0	0.99
f656n	3	-81.9	098	56500	94.4	85.2	0.98
f656n	3	-81.7	104	58003	95.0	85.3	0.98
f657n	3	-81.7	088	54268	732.6	691.2	1.00
f657n	3	-81.7	096	56211	727.7	683.8	0.99
f657n	3	-81.5	099	56790	719.7	678.3	0.98
f658n	3	-81.9	086	53849	247.9	223.3	1.00
f658n	3	-81.9	093	55575	245.4	222.2	0.99
f658n	3	-81.7	098	56522	243.8	221.1	0.99
f658n	3	-81.7	104	58004	242.2	219.6	0.98
f665n	3	-82.3	088	54267	818.0	736.0	1.00
f665n	3	-81.9	096	56210	809.9	728.2	0.99
f665n	3	-81.9	099	56789	803.2	723.5	0.98
f673n	3	-82.1	086	53841	787.6	710.0	1.00
f673n	3	-81.5	093	55564	778.1	703.9	0.99
f673n	3	-81.7	098	56511	770.7	698.4	0.98
f680n	3	-82.1	088	54266	2719.4	2461.8	1.00
f680n	3	-81.9	096	56209	2701.8	2437.5	0.99

filter	L	iuv-detmp	doy	tvnum	median (e^-/s/p)		ratio
					chip1	chip2	
f438w	1	-82.1	073	51263	119.5	107.8	1.00
f438w	1	-81.9	089	54335	114.6	103.5	0.96
f438w	1	-81.9	103	57876	118.2	106.4	0.99
f438w	2	-81.7	103	57877	135.0	120.0	1.00
f438w	3	-81.7	078	52443	139.4	124.9	1.00
f438w	3	-81.7	078	52443	139.4	124.9	1.00
f438w	3	-81.9	093	55514	137.8	123.0	0.99
f438w	3	-81.9	093	55514	137.8	123.0	0.99
f438w	3	-81.7	098	56502	135.9	121.3	0.97
f438w	3	-81.7	098	56502	135.9	121.3	0.97
f438w	3	-81.7	103	57882	135.8	121.1	0.97
f438w	3	-81.7	103	57882	135.8	121.1	0.97
f438w	4	-81.9	103	57883	156.6	141.5	1.00
f467m	3	-82.1	086	53851	105.6	94.7	1.00
f467m	3	-82.1	086	53851	105.6	94.7	1.00
f467m	3	-81.9	093	55577	104.4	93.5	0.99
f467m	3	-81.9	093	55577	104.4	93.5	0.99
f467m	3	-81.9	098	56524	103.0	92.6	0.98
f467m	3	-81.9	098	56524	103.0	92.6	0.98
f469n	3	-82.3	086	53842	19.2	17.4	1.00
f469n	3	-81.9	093	55565	18.9	0.0	0.00
f469n	3	-81.7	098	56512	18.7	17.0	0.98
f475w	3	-82.3	078	52454	1016.2	911.8	1.00
f475w	3	-81.7	093	55664	1006.3	901.8	0.99
f475w	3	-81.7	099	56758	994.6	890.9	0.98
f475w	3	-81.7	104	57997	987.4	885.3	0.97
f475x	3	-81.7	078	52449	2763.3	2476.4	1.00
f475x	3	-81.7	093	55659	2723.5	2447.8	0.99
f475x	3	-81.9	099	56753	2695.7	2419.5	0.98
f475x	3	-81.7	104	57998	2695.6	2426.7	0.98
f487n	3	-81.7	086	53852	40.8	36.9	1.00
f487n	3	-82.1	093	55578	40.2	36.5	0.99
f487n	3	-81.7	098	56525	39.9	36.0	0.98
f502n	3	-82.1	086	53844	58.1	52.2	1.00
f502n	3	-81.9	093	55567	57.2	51.6	0.99
f502n	3	-81.7	098	56514	56.7	51.2	0.98
f547m	3	-82.1	086	53837	1180.2	1058.3	1.00
f547m	3	-81.7	093	55559	1134.2	1015.7	0.96
f547m	3	-81.9	098	56506	1125.1	1008.0	0.95
f555w	1	-81.7	066	49262	2502.4	2263.5	1.00
f555w	1	-81.1	067	49351	2524.5	2290.9	1.01
f555w	1	-81.9	073	51262	2566.9	2325.4	1.03
f555w	1	-81.7	079	52561	2568.3	2327.6	1.03
f555w	1	-81.3	082	52887	2473.8	2237.6	0.99
f555w	1	-81.7	083	52925	2509.3	2284.6	1.01
f555w	1	-82.1	089	54467	2506.8	2271.4	1.00
f555w	1	-81.5	097	56333	2497.1	2267.3	1.00
f555w	1	-81.9	103	57875	2548.3	2315.3	1.02
f555w	1	-81.7	104	58032	2548.8	2315.7	1.02
f555w	2	-81.5	103	57878	3074.8	2749.2	1.00
f680n	3	-81.7	099	56788	2665.3	2419.3	0.98
f689m	3	-82.1	086	53843	5021.5	4508.7	1.00
f689m	3	-81.9	093	55566	4965.7	4474.3	0.99
f689m	3	-81.9	098	56513	4923.7	4436.0	0.98
f763m	3	-82.3	086	53845	7284.4	6619.6	1.00
f763m	3	-82.3	086	53845	7284.4	6619.6	1.00
f763m	3	-82.1	093	55568	7213.4	6562.8	0.99
f763m	3	-82.1	093	55568	7213.4	6562.8	0.99
f763m	3	-81.7	098	56515	7147.1	6524.7	0.98
f763m	3	-81.7	098	56515	7147.1	6524.7	0.98
f775w	3	-82.3	078	52452	13767.0	12471.8	1.00
f775w	3	-82.1	093	55662	13595.6	12382.1	0.99
f775w	3	-81.9	099	56756	13468.4	12289.6	0.98
f775w	3	-82.1	104	58005	13483.8	12299.1	0.98
f814w	1	-81.7	066	49263	19022.0	17680.9	1.00
f814w	1	-81.7	066	49263	19022.0	17680.9	1.00
f814w	1	-81.3	067	49352	19104.5	17752.6	1.00
f814w	1	-81.3	067	49352	19104.5	17752.6	1.00
f814w	1	-82.1	073	51264	19020.0	17651.1	1.00
f814w	1	-82.1	073	51264	19020.0	17651.1	1.00
f814w	1	-82.1	079	52562	19065.0	17736.7	1.00
f814w	1	-82.1	079	52562	19065.0	17736.7	1.00
f814w	1	-81.1	082	52888	18719.0	17419.2	0.98
f814w	1	-81.1	082	52888	18719.0	17419.2	0.98
f814w	1	-81.7	083	52926	18806.8	17533.2	0.99
f814w	1	-81.7	083	52926	18806.8	17533.2	0.99
f814w	1	-82.3	089	54336	18723.3	17408.2	0.98
f814w	1	-82.3	089	54336	18723.3	17408.2	0.98
f814w	1	-81.7	089	54468	18776.8	17421.1	0.99
f814w	1	-81.7	089	54468	18776.8	17421.1	0.99
f814w	1	-81.7	097	56334	18805.9	17489.1	0.99
f814w	1	-81.7	097	56334	18805.9	17489.1	0.99
f814w	1	-81.5	103	57874	18438.2	17109.2	0.97
f814w	1	-81.5	103	57874	18438.2	17109.2	0.97
f814w	1	-81.9	104	58033	19054.5	17724.6	1.00
f814w	1	-81.9	104	58033	19054.5	17724.6	1.00
f814w	2	-81.7	103	57879	24050.5	22032.4	1.00
f814w	3	-81.5	078	52439	21305.7	19561.7	1.00
f814w	3	-81.5	078	52439	21305.7	19561.7	1.00
f814w	3	-81.5	078	52439	21305.7	19561.7	1.00
f814w	3	-81.7	093	55510	21189.7	19517.1	1.00
f814w	3	-81.7	093	55510	21189.7	19517.1	1.00
f814w	3	-81.7	093	55510	21189.7	19517.1	1.00
f814w	3	-81.5	098	56498	20883.4	19241.0	0.98
f814w	3	-81.5	098	56498	20883.4	19241.0	0.98
f814w	3	-81.5	098	56498	20883.4	19241.0	0.98
f814w	3	-81.9	103	57880	20879.8	19182.0	0.98
f814w	3	-81.9	103	57880	20879.8	19182.0	0.98
f814w	3	-81.9	103	57880	20879.8	19182.0	0.98
f814w	4	-81.9	103	57885	25140.3	23455.6	1.00

filter	L	iuv-detmp	doy	tvnum	median (e^-/s/p)		ratio
					chip1	chip2	
f555w	3	-82.1	078	52440	2991.3	2681.5	1.00
f555w	3	-81.5	093	55511	2945.3	2653.1	0.99
f555w	3	-81.9	098	56499	2914.8	2626.3	0.98
f555w	3	-81.7	103	57881	2935.0	2635.8	0.98
f555w	4	-82.1	103	57884	3400.5	3081.4	1.00
f600lp	3	-81.7	086	53850	32486.3	29782.8	1.00
f600lp	3	-81.7	093	55576	32142.0	29580.7	0.99
f600lp	3	-81.7	098	56523	31723.1	29216.6	0.98
f600lp	3	-82.1	104	57999	31655.0	29084.0	0.98

filter	L	iuv-detmp	doy	tvnum	median (e^-/s/p)		ratio
					chip 1	chip 2	
f845m	3	-82.1	086	53847	8399.3	7635.5	1.00
f845m	3	-82.1	093	55572	8093.8	7361.7	0.96
f845m	3	-81.7	098	56519	8000.2	7314.1	0.96
f850lp	3	-81.9	078	52453	11595.4	10828.9	1.00
f850lp	3	-82.1	093	55663	11522.5	10759.6	0.99
f850lp	3	-81.7	099	56757	11496.2	10727.1	0.99
f953n	3	-82.1	078	52442	556.0	536.1	1.00
f953n	3	-81.9	093	55513	552.7	532.6	0.99
f953n	3	-81.7	098	56501	548.9	531.4	0.99
f953n	3	-81.7	104	58006	548.9	531.9	0.99

Table 4. UVIS tungsten lamp exposure levels in quad filters, all taken with lamp 3 and IUVDETMP of -82C. Listed are filter name, amp, filter keyword from the image header, instrument side, number of images, mean and median count-rates, as measured from the central 1000x1000 pixels in the quadrant noted, and standard deviation. All count-rates have been converted to e^- using a gain of 1.5 e^-/DN.

filter name	amp	filter keyword	side	num images	mean (e^-/s/p)	sdev	median (e^-/s/p)
fq508n	A	quad	both	9	113.1	1.2	113.1
fq674n	B		both	9	85.3	0.7	85.4
fq575n	C		both	9	41.9	0.4	42.0
fq672n	D		both	9	134.7	1.1	134.8
fq437n	A	quad1	both	3	6.0	0.1	6.0
fq378n	B		both	3	4.6	0.1	4.6
fq232n	C		both	3	1.6	0.0	1.6
fq243n	D		both	3	1.5	0.0	1.5
fq387n	A	quad2	both	27	1.8	0.0	1.8
fq492n	B		both	27	80.9	0.8	80.9
fq422m	C		both	27	12.6	0.2	12.6
fq436n	D		both	27	8.9	0.1	8.9
fq889n	A	quad3	both	3	729.3	3.3	729.8
fq937n	B		both	3	652.5	3.1	652.6
fq906n	C		both	3	734.6	3.9	733.8
fq924n	D		both	3	734.1	3.8	734.7
fq619n	A	quad4	both	10	229.5	3.3	229.4
fq750n	B		both	10	571.5	8.7	572.6

filter name	amp	filter keyword	side	num images	mean (e^-/s/p)	sdev	median (e^-/s/p)
fq634n	C		both	10	285.7	4.3	285.9
fq727n	D		both	10	557.2	8.0	557.4
			separated by MEB				
fq387n	A	quad2	meb1	9	1.8	0.0	1.8
fq387n	A		meb2	18	1.8	0.0	1.8
fq492n	B		meb	9	81.8	0.3	81.9
fq492n	B		meb2	18	80.4	0.5	80.2
fq422m	C		meb1	9	12.8	0.0	12.8
fq422m	C		meb2	18	12.5	0.1	12.5
fq436n	D		meb1	9	9.0	0.0	9.1
fq436n	D		meb2	18	8.9	0.1	8.8
fq619n	A	quad4	meb1	4	230.7	3.7	230.5
fq619n	A		meb2	6	228.7	3.1	229.4
fq750n	B		meb1	4	573.3	10.6	573.2
fq750n	B		meb2	6	570.3	8.1	572.6
fq634n	C		meb1	4	287.2	4.8	287.2
fq634n	C		meb2	6	284.7	4.0	285.9
fq727n	D		meb1	4	559.5	9.2	559.5
fq727n	D		meb2	6	555.6	7.7	557.4

Table 5. UVIS deuterium full-frame flatfield count-rates from TV3. Listed are filtername, instrument side, CCD temperature as given by the IUVDETMP header keyword, day of year that the image was taken, TV number of the image, median count-rates in chip 1 (quads A/B), in chip2 (quads C/D), and flux ratio of the flat as referenced to the first flat taken in that filter/lamp/temperature group. All count-rates have been converted to e^- using a gain of 1.5 e^-/DN. See Table 7 for exposure levels for specific quadrants of the quad filters.

filter	side	iuv detmp	DOY	tvnum	median (e^-/s/p)		ratio
					chip 1	chip 2	
f200lp	meb1	-82.1	078	52433	11894.8	9952.2	1.00
f200lp	meb1	-81.9	089	54447	11226.3	9382.6	0.94
f200lp	meb1	-81.7	089	54448	11275.2	9419.7	0.95
f200lp	meb2	-81.9	096	56269	11026.1	9205.6	0.93
f200lp	meb2	-81.7	096	56270	11044.2	9196.9	0.93
f218w	meb1	-49.4	054	49074	939.1	714.0	0.97
f218w	meb2	-81.9	066	49264	981.3	730.5	1.00
f218w	meb1	-81.5	067	49353	973.7	725.1	0.99
f218w	meb1	-81.7	078	52431	964.6	719.1	0.98
f218w	meb1	-81.9	079	52563	952.7	709.4	0.97
f218w	meb2	-81.1	082	52889	951.2	709.5	0.97
f218w	meb1	-81.7	083	52927	948.4	705.5	0.97
f218w	meb1	-81.7	089	54443	914.0	681.1	0.93
f218w	meb1	-82.1	089	54444	915.9	682.3	0.93
f218w	meb1	-82.1	089	54469	908.1	675.0	0.92
f218w	meb2	-81.9	096	56265	890.5	663.0	0.91
f218w	meb2	-81.7	096	56266	892.0	663.3	0.91
f218w	meb2	-81.7	097	56335	890.4	661.6	0.91
f218w	meb2	-81.7	104	58034	892.0	662.7	0.91
f225w	meb1	-82.3	078	52427	1955.0	1496.3	1.00
f225w	meb1	-81.7	089	54433	1916.1	1463.0	0.98
f225w	meb1	-82.3	089	54434	1985.2	1538.3	1.02
f225w	meb1	-82.1	089	54436	1994.7	1543.5	1.03
f225w	meb2	-81.9	096	56256	0.0	0.0	0.00
f225w	meb2	-81.5	096	56257	1932.8	1495.5	0.99
f225w	meb2	-81.9	096	56258	1937.5	1499.1	1.00
f225w	meb2	-81.9	096	56276	1882.4	1455.9	0.97
f275w	meb1	-81.9	078	52419	1086.7	988.5	1.00
f275w	meb1	-81.7	089	54322	1027.1	932.2	0.94
f275w	meb1	-82.1	089	54323	1030.2	932.2	0.95
f275w	meb2	-81.7	096	56193	996.6	903.2	0.92
f275w	meb2	-81.5	096	56194	997.6	904.0	0.92
f280n	meb1	-82.1	078	52432	43.6	41.8	1.00
f280n	meb1	-81.9	089	54445	41.2	39.5	0.94
f336w	meb1	-81.7	078	52417	626.4	602.4	1.00
f336w	meb1	-82.1	088	54318	594.9	572.8	0.95
f336w	meb1	-82.1	088	54319	595.8	572.3	0.95
f336w	meb2	-81.9	096	56189	580.1	556.7	0.93
f336w	meb2	-81.9	096	56190	579.7	556.0	0.92
f336w	meb1	-81.7	087	54178	583.1	0.0	1.00
f336w	meb1	-81.7	087	54179	583.3	0.0	1.00
f336w	meb1	-82.1	087	54180	587.8	0.0	1.01
f336w	meb1	-82.1	087	54181	587.9	0.0	1.01
f336w	meb1	-82.1	087	54182	589.3	0.0	1.01
f336w	meb1	-82.1	087	54183	589.4	0.0	1.01
f336w	meb1	-82.1	087	54184	590.4	0.0	1.01
f336w	meb1	-82.1	087	54185	590.2	0.0	1.01
f336w	meb1	-81.9	087	54186	591.6	0.0	1.01
f336w	meb1	-82.1	087	54187	591.5	0.0	1.01
f336w	meb1	-81.7	087	54188	592.4	0.0	1.02
f336w	meb1	-81.9	087	54189	592.5	0.0	1.02
f343n	meb1	-82.1	078	52421	259.9	248.8	1.00
f343n	meb1	-81.7	089	54326	247.4	236.6	0.95
f343n	meb1	-81.9	089	54327	247.9	237.1	0.95
f343n	meb2	-81.9	096	56197	240.3	229.4	0.92
f343n	meb2	-81.9	096	56198	240.7	229.2	0.92
f373n	meb1	-82.3	078	52428	27.9	26.9	1.00
f373n	meb1	-82.3	089	54437	27.0	26.1	0.97
f373n	meb1	-81.9	089	54438	27.0	26.0	0.97
f373n	meb2	-81.9	096	56259	26.3	25.4	0.94
f373n	meb2	-81.7	096	56260	26.4	25.5	0.95
f390m	meb1	-82.1	078	52423	132.8	128.9	1.00
f390m	meb1	-82.1	089	54330	127.0	123.4	0.96
f390m	meb1	-82.3	089	54331	127.2	123.6	0.96
f390m	meb2	-81.9	096	56201	123.3	119.9	0.93
f390m	meb2	-81.7	096	56202	123.7	120.0	0.93
f390w	meb1	-82.1	078	52429	659.7	641.3	1.00
f390w	meb1	-82.1	089	54439	627.8	609.5	0.95

filter	side	iuv detmp	DOY	tvnum	median (e^-/s/p)		ratio
					chip 1	chip 2	
f280n	meb1	-81.7	089	54446	41.3	39.6	0.95
f280n	meb2	-81.9	096	56267	40.2	38.5	0.92
f280n	meb2	-81.9	096	56268	40.3	38.5	0.92
f300x	meb1	-81.7	078	52415	0.0	-0.0	0.00
f300x	meb1	-82.1	078	52425	2154.6	1908.2	1.00
f300x	meb1	-82.1	088	54313	-0.0	0.0	-0.00
f300x	meb1	-81.9	088	54314	2129.5	1889.9	0.99
f300x	meb1	-81.9	088	54315	2140.6	1899.0	0.99
f300x	meb1	-82.1	089	54333	2059.3	1826.3	0.96
f300x	meb1	-81.7	089	54334	2107.9	1870.2	0.98
f300x	meb2	-81.9	096	56184	2092.7	1831.6	0.97
f300x	meb2	-81.7	096	56185	2084.0	1846.6	0.97
f300x	meb2	-81.7	096	56186	2093.0	1849.4	0.97

filter	side	iuv detmp	DOY	tvnum	median (e^-/s/p)		ratio
					chip 1	chip 2	
f390w	meb1	-81.7	089	54440	627.8	608.3	0.95
f390w	meb2	-81.7	096	56261	613.9	594.8	0.93
f390w	meb2	-81.9	096	56262	614.8	595.4	0.93
f395n	meb1	-81.9	078	52420	55.2	54.1	1.00
f395n	meb1	-81.9	089	54324	52.5	51.6	0.95
f395n	meb1	-82.1	089	54325	52.7	51.6	0.95
f395n	meb2	-81.7	096	56195	51.2	50.2	0.93
f395n	meb2	-81.5	096	56196	51.4	50.3	0.93

Table 6. UVIS deuterium subarray flatfields, all positioned in amp C on chip 1; columns are the same as Table 5.

filter	side	iuv-detmp	DOY	tvnum	median chip 1 (e^-/s/p)	ratio
f218w	meb1	-82.1	087	54142	-0.0	-0.00
f218w	meb1	-81.7	087	54143	0.5	0.00
f218w	meb1	-81.9	087	54144	0.0	0.00
f218w	meb1	-81.9	087	54145	-0.0	-0.00
f218w	meb1	-81.7	087	54146	0.0	0.00
f218w	meb1	-81.9	087	54147	913.9	1.00
f218w	meb1	-81.9	087	54148	912.8	1.00
f218w	meb1	-82.3	087	54149	909.1	0.99
f218w	meb1	-82.1	087	54150	910.0	1.00
f218w	meb1	-82.1	087	54151	914.3	1.00
f218w	meb1	-81.9	087	54152	921.6	1.01
f218w	meb1	-82.1	087	54153	927.6	1.02
f218w	meb1	-82.1	087	54203	888.5	0.97
f218w	meb1	-82.1	087	54204	911.4	1.00
f218w	meb1	-81.7	087	54205	911.9	1.00
f218w	meb1	-81.9	087	54206	912.6	1.00
f218w	meb1	-82.1	087	54207	916.2	1.00
f218w	meb1	-82.1	087	54208	916.6	1.00

filter	side	iuv-detmp	DOY	tvnum	median chip 1 (e^-/s/p)	ratio
f225w	meb1	-82.1	087	54154	1883.8	1.00
f225w	meb1	-82.1	087	54155	1904.8	1.01
f225w	meb1	-81.7	087	54156	1986.1	1.05
f225w	meb1	-81.7	087	54157	1984.4	1.05
f225w	meb1	-82.1	087	54158	1996.4	1.06
f225w	meb1	-82.1	087	54159	2000.6	1.06
f225w	meb1	-81.7	087	54160	2000.5	1.06
f225w	meb1	-82.3	087	54161	2000.9	1.06
f225w	meb1	-81.9	087	54162	2003.4	1.06
f225w	meb1	-82.1	087	54163	2005.7	1.06
f225w	meb1	-81.9	087	54164	2006.1	1.06
f225w	meb1	-81.7	087	54165	2005.4	1.06
f275w	meb1	-82.1	087	54166	999.4	1.00
f275w	meb1	-81.9	087	54167	1009.2	1.01
f275w	meb1	-82.1	087	54168	1008.7	1.01
f275w	meb1	-82.1	087	54169	1011.4	1.01
f275w	meb1	-82.1	087	54170	1014.9	1.02
f275w	meb1	-82.3	087	54171	1014.4	1.01
f275w	meb1	-82.3	087	54172	1015.9	1.02
f275w	meb1	-82.1	087	54173	1015.5	1.02
f275w	meb1	-81.7	087	54174	1017.8	1.02
f275w	meb1	-82.1	087	54175	1016.9	1.02
f275w	meb1	-81.9	087	54176	1019.1	1.02
f275w	meb1	-82.1	087	54177	1017.9	1.02

Table 7. UVIS deuterium lamp quad filter count-rates from TV3. Columns are the same as in Table 5, except that statistics are from central 400x400 region in each quad.

filter	exptime	side	DOY	tvnum	median (e^-/s/p)	ratio	filter	exptime	side	DOY	tvnum	median (e^-/s/p)	ratio
fq232n	475.	meb1	78	52416	58.4	1.00	fq422m	860.	meb1	78	52430	42.6	1.00
fq232n	475.	meb1	78	52418	59.3	1.01	fq422m	860.	meb1	78	52434	42.4	1.00
fq232n	475.	meb1	78	52422	58.7	1.00	fq422m	860.	meb1	78	52435	42.3	0.99
fq232n	237.5	meb1	88	54316	56.0	0.96	fq422m	430.	meb1	89	54441	40.5	0.95
fq232n	475.	meb1	88	54317	56.1	0.96	fq422m	860.	meb1	89	54442	40.6	0.95
fq232n	237.5	meb1	89	54320	55.7	0.95	fq422m	430.	meb1	89	54449	40.3	0.95
fq232n	475.	meb1	89	54321	55.8	0.96	fq422m	430.	meb1	89	54450	40.3	0.95
fq232n	237.5	meb1	89	54328	55.4	0.95	fq422m	860.	meb1	89	54451	40.4	0.95
fq232n	475.	meb1	89	54329	55.6	0.95	fq422m	860.	meb1	89	54452	40.4	0.95
fq232n	237.5	meb2	96	56187	54.3	0.93	fq422m	430.	meb2	96	56263	39.6	0.93
fq232n	475.	meb2	96	56188	54.4	0.93	fq422m	860.	meb2	96	56264	39.7	0.93
fq232n	237.5	meb2	96	56191	53.9	0.92	fq422m	430.	meb2	96	56271	39.4	0.92
fq232n	475.	meb2	96	56192	54.1	0.93	fq422m	430.	meb2	96	56272	39.4	0.92
fq232n	237.5	meb2	96	56199	53.5	0.92	fq422m	860.	meb2	96	56273	39.5	0.93
fq232n	475.	meb2	96	56200	53.6	0.92	fq422m	860.	meb2	96	56274	39.5	0.93
fq243n	475.	meb1	78	52416	69.1	1.00	fq436n	860.	meb1	78	52430	14.8	1.00
fq243n	475.	meb1	78	52418	69.9	1.01	fq436n	860.	meb1	78	52434	14.7	0.99
fq243n	475.	meb1	78	52422	69.3	1.00	fq436n	860.	meb1	78	52435	14.7	0.99
fq243n	237.5	meb1	88	54316	66.6	0.96	fq436n	430.	meb1	89	54441	14.2	0.96
fq243n	475.	meb1	88	54317	66.7	0.96	fq436n	860.	meb1	89	54442	14.2	0.96
fq243n	237.5	meb1	89	54320	66.3	0.96	fq436n	430.	meb1	89	54449	14.1	0.95
fq243n	475.	meb1	89	54321	66.4	0.96	fq436n	430.	meb1	89	54450	14.1	0.95
fq243n	237.5	meb1	89	54328	66.0	0.95	fq436n	860.	meb1	89	54451	14.2	0.96
fq243n	475.	meb1	89	54329	66.1	0.96	fq436n	860.	meb1	89	54452	14.2	0.96
fq243n	237.5	meb2	96	56187	64.9	0.94	fq436n	430.	meb2	96	56263	14.0	0.94
fq243n	475.	meb2	96	56188	64.9	0.94	fq436n	860.	meb2	96	56264	14.0	0.94
fq243n	237.5	meb2	96	56191	64.5	0.93	fq436n	430.	meb2	96	56271	13.9	0.94
fq243n	475.	meb2	96	56192	64.5	0.93	fq436n	430.	meb2	96	56272	13.9	0.94
fq243n	237.5	meb2	96	56199	64.0	0.93	fq436n	860.	meb2	96	56273	13.9	0.94
fq243n	475.	meb2	96	56200	64.1	0.93	fq436n	860.	meb2	96	56274	13.9	0.94

filter	exptime	side	DOY	tvnum	median (e^-/s/p)	ratio
fq378n	475.	meb1	78	52416	57.1	1.00
fq378n	475.	meb1	78	52418	58.8	1.03
fq378n	475.	meb1	78	52422	58.3	1.02
fq378n	237.5	meb1	88	54316	56.4	0.99
fq378n	475.	meb1	88	54317	56.5	0.99
fq378n	237.5	meb1	89	54320	56.1	0.98
fq378n	475.	meb1	89	54321	56.2	0.98
fq378n	237.5	meb1	89	54328	55.9	0.98
fq378n	475.	meb1	89	54329	56.0	0.98
fq378n	237.5	meb2	96	56187	55.2	0.97
fq378n	475.	meb2	96	56188	55.2	0.97
fq378n	237.5	meb2	96	56191	54.9	0.96
fq378n	475.	meb2	96	56192	54.9	0.96
fq378n	237.5	meb2	96	56199	54.5	0.95
fq378n	475.	meb2	96	56200	54.6	0.96
fq387n	860.	meb1	78	52430	17.3	1.00
fq387n	860.	meb1	78	52434	17.2	1.00
fq387n	860.	meb1	78	52435	17.2	1.00
fq387n	430.	meb1	89	54441	16.4	0.95
fq387n	860.	meb1	89	54442	16.4	0.95
fq387n	430.	meb1	89	54449	16.3	0.95
fq387n	430.	meb1	89	54450	16.4	0.95
fq387n	860.	meb1	89	54451	16.4	0.95
fq387n	860.	meb1	89	54452	16.3	0.95
fq387n	430.	meb2	96	56263	16.0	0.93
fq387n	860.	meb2	96	56264	16.0	0.93
fq387n	430.	meb2	96	56271	16.0	0.92
fq387n	430.	meb2	96	56272	15.9	0.92
fq387n	860.	meb2	96	56273	16.0	0.92
fq387n	860.	meb2	96	56274	15.9	0.92

filter	exptime	side	DOY	tvnum	median (e^-/s/p)	ratio
fq437n	475.	meb1	78	52416	11.2	1.00
fq437n	475.	meb1	78	52418	11.4	1.01
fq437n	475.	meb1	78	52422	11.3	1.01
fq437n	237.5	meb1	88	54316	10.9	0.97
fq437n	475.	meb1	88	54317	10.9	0.97
fq437n	237.5	meb1	89	54320	10.8	0.96
fq437n	475.	meb1	89	54321	10.8	0.96
fq437n	237.5	meb1	89	54328	10.8	0.96
fq437n	475.	meb1	89	54329	10.8	0.96
fq437n	237.5	meb2	96	56187	10.6	0.95
fq437n	475.	meb2	96	56188	10.6	0.95
fq437n	237.5	meb2	96	56191	10.6	0.94
fq437n	475.	meb2	96	56192	10.6	0.94
fq437n	237.5	meb2	96	56199	10.5	0.94
fq437n	475.	meb2	96	56200	10.5	0.94
fq492n	860.	meb1	78	52430	25.6	1.00
fq492n	860.	meb1	78	52434	25.5	0.99
fq492n	860.	meb1	78	52435	25.4	0.99
fq492n	430.	meb1	89	54441	24.7	0.96
fq492n	860.	meb1	89	54442	24.6	0.96
fq492n	430.	meb1	89	54449	24.6	0.96
fq492n	430.	meb1	89	54450	24.5	0.96
fq492n	860.	meb1	89	54451	24.5	0.96
fq492n	860.	meb1	89	54452	24.5	0.96
fq492n	430.	meb2	96	56263	24.3	0.95
fq492n	860.	meb2	96	56264	24.3	0.95
fq492n	430.	meb2	96	56271	24.1	0.94
fq492n	430.	meb2	96	56272	24.1	0.94
fq492n	860.	meb2	96	56273	24.2	0.94
fq492n	860.	meb2	96	56274	24.1	0.94